

# Manifold configurations of the director field formed by topological defects in free and confined geometry in smectic films

P. V. Dolganov<sup>1</sup> and P. Cluzeau<sup>2</sup><sup>1</sup>*Institute of Solid State Physics, RAS, 142432, Chernogolovka, Moscow Region, Russia*<sup>2</sup>*Université de Bordeaux, Centre de Recherche Paul Pascal, CNRS, Avenue A. Schweitzer, 33600 Pessac, France*

(Received 10 March 2014; revised manuscript received 26 September 2014; published 1 December 2014)

We study the topology of the  $\mathbf{c}$ -director field near topological defects with point core and with a droplet in the core of the defect in nonpolar smectic- $C$  and ferroelectric smectic- $C^*$  freestanding films using polarized optical microscopy. Free and confined geometry of topological defects and droplets with strong outer boundary condition are compared. The  $\mathbf{c}$ -director field can be remarkably different around a point defect and a droplet with the same topological charge  $S = +1$ . In ferroelectric films, splay deformation of the  $\mathbf{c}$ -director transforms into bend deformation after droplet nucleation. Heating a ferroelectric film with an  $S = +1$  droplet leads to a dramatic change of the  $\mathbf{c}$ -director topology from bend to splay. In confined geometry we found spiral structures in which the  $\mathbf{c}$ -director has opposite direction of rotation along the inner and outer boundaries of the island. Our observations are discussed on the basis of theories taking into account both the influence of polarity and of confined geometry on elasticity and topology of the  $\mathbf{c}$ -director field.

DOI: [10.1103/PhysRevE.90.062501](https://doi.org/10.1103/PhysRevE.90.062501)

PACS number(s): 61.30.Jf, 61.30.Hn, 81.16.Dn

Topological defects in liquid crystals are nontrivial objects that are interesting by themselves, and their investigation also allows us to obtain qualitative and quantitative information about the system [1,2]. In this paper, we report studies of topological defects in thin freestanding films of achiral smectic- $C$  (SmC) and chiral smectic- $C^*$  (SmC\*) liquid crystals [1]. In these phases the molecules are tilted in the smectic layers. The projection of the long molecular axis onto the layer plane defines the two-dimensional (2D)  $\mathbf{c}$ -director field [1,2]. In ferroelectric SmC\* films the polarization  $\mathbf{P}$  is perpendicular to  $\mathbf{c}$ . In freestanding films the layer planes are parallel to the free surfaces. Films can be prepared with thickness from two to hundreds of molecular layers [3]. The topological defects in the films can be generated both at phase transitions and by a strong action on the film when continuous  $\mathbf{c}$ -director field is broken. In experiments by Link *et al.* [4], different structures of topological defects were observed in anticlinic films with antiferroelectric SmC<sub>A</sub>\* phase. Polarization in anticlinic films depends on the oddness of number of layers. Circular  $\mathbf{c}$ -director orientation near defects with topological charge  $S = +1$  was found in the films with an even number of layers (low polarization), radial orientation in films with an odd number of layers (high polarization). Moreover, transformation of the  $\mathbf{c}$ -director configuration was found near droplet-defect pairs (topological dipoles) [5,6]. Nontrivial results of studies of the topological defects in antiferroelectric films [4], in smectic islands in SmC\* films [7], and in the topological dipoles and quadrupoles [5,6,8–10] were an important motivation for our investigations of transformation of the  $\mathbf{c}$ -director field near topological defects in nonpolar and polar films.

In this paper, we studied in polar and nonpolar freestanding films defects with a core containing a nematic ( $N$ ) or a cholesteric ( $N^*$ ) droplet. Such droplets can nucleate in the center of topological defect on heating. We observed dramatic transformations of the director field around the droplets in ferroelectric films. With temperature, the boundary conditions change between tangential (the  $\mathbf{c}$ -director parallel to droplet boundary) and radial (the  $\mathbf{c}$ -director perpendicular to droplet

boundary) through a rotation of the  $\mathbf{c}$ -director by  $90^\circ$  at the droplet boundary. We also observed and described the configurations of the  $\mathbf{c}$ -director around droplets in confined geometry of smectic islands. The observed  $\mathbf{c}$ -director configurations are driven by the competition between elasticity, polarity, and anchoring energy at the droplet boundary. The influence of these parameters will be discussed in this paper.

The measurements were made on chiral ferroelectric compounds 4'-nonylxybiphenyl-4-yl 4-(1-methylheptyloxy)benzoate (9BSMHOB), 4'-undecyloxybiphenyl-4-yl 4-(1-methylheptyloxy)benzoate (11BSMHOB) [11] and on nonchiral compounds 4-decyloxy-benzoic acid (DOBA) [12], 4-hexyloxyphenyl-4'-decyloxybenzoate (HOPDOB) [13]. 9BSMHOB has the following phase sequence: K-(56.8 °C)-SmC\*-(104.6 °C)-N\*-(131.4 °C)-Isotropic ( $I$ ). In 11BSMHOB the phase sequence is K-(56.5 °C)-SmC\*-(108 °C)-N\*-(124 °C)- $I$ . In freestanding films the nucleation of droplets begins above bulk SmC- $N$  or SmC\*- $N^*$  transitions [6]. The polarization  $P$  of chiral compounds in SmC\* is about 120 esu/cm<sup>2</sup> [11]. Freestanding films were prepared by drawing a small amount of the material in the smectic state across a 3-mm circular hole in a glass plate or using a rectangular frame with two mobile blades. The topological defects in the films were observed with an optical microscope in the reflection mode. Observations were made with crossed polarizers and with polarizers slightly decrossed [14]. Usage of decrossed polarizers allows determining the director orientation. Images were taken with a charge-coupled device (CCD) camera.

The director field around point defects has been extensively studied in the past [4,15–22]. Orientation of the  $\mathbf{c}$ -director near  $S = +1$  defects can be both circular and radial. Figures 1(a) and 2(a) show point topological defects in nonpolar SmC and ferroelectric SmC\* freestanding films. Both singularities in the  $\mathbf{c}$ -director field are topological defects with the same charge  $S = +1$ . In the SmC films circular orientation of the  $\mathbf{c}$ -director is observed [Fig. 1(b)], whereas in ferroelectric SmC\* films the  $\mathbf{c}$ -director orientation is radial [Fig. 2(b)]. While this result is not new [19], let us discuss this difference in

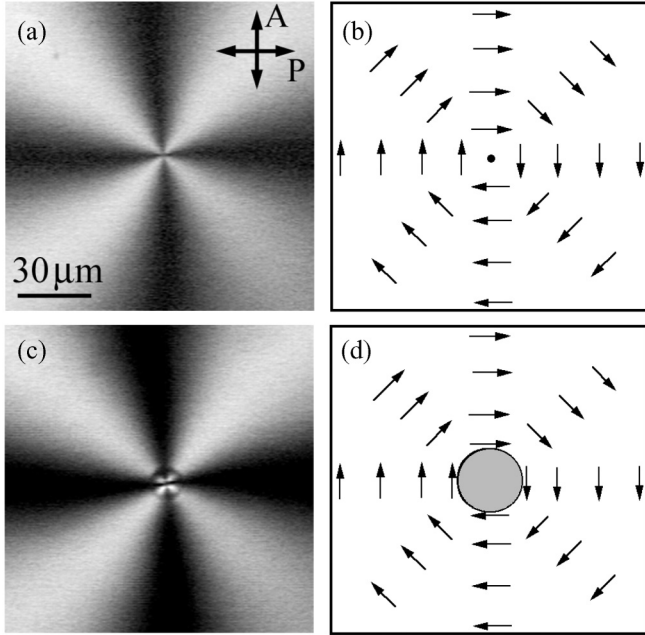


FIG. 1. A nonpolar SmC freestanding film. (a) A point topological defect with topological charge  $S = +1$ ,  $T = 112^\circ\text{C}$ . The topological defect (c) after nucleation of a nematic droplet in the core of the defect,  $T = 115^\circ\text{C}$ , DOBA. The photographs were made under crossed polarizers (P, A). A schematic representation of the  $\mathbf{c}$ -director configuration around the topological defect (b) and the droplet (d).

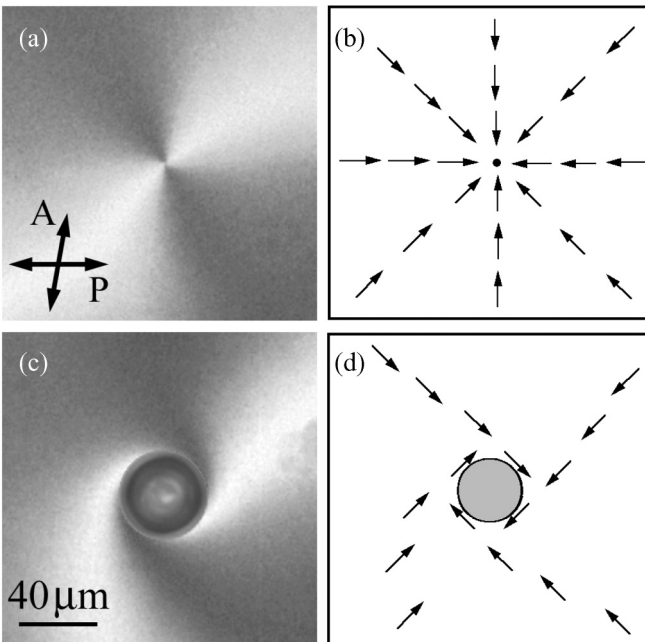


FIG. 2. A ferroelectric SmC\* freestanding film. (a) A point defect with topological charge  $S = +1$ . The topological defect (c) after nucleation of a cholesteric droplet in the core of the defect on heating,  $T = 109^\circ\text{C}$ , 11BSMHOB. The photographs were made under slightly decrossed polarizers (P, A). A schematic representation of the  $\mathbf{c}$ -director configuration around the topological defect (b) and the droplet (d).

more detail in order to better understand our forthcoming more complex experimental results for the droplets and the change of the  $\mathbf{c}$ -director orientation near the droplets on heating. The configurations corresponding to the minimum of the energy will be realized in the film. Generally, the elastic energy over the film is written as [23]

$$F_{el} = h \int \left( \frac{K_S}{2} (\nabla \cdot \mathbf{c})^2 + \frac{K_B}{2} (\nabla \times \mathbf{c})^2 \right) d^2x, \quad (1)$$

where  $K_S$  and  $K_B$ , respectively, are the 2D splay and bend elastic constants, and  $h$  is the film thickness. The  $\mathbf{c}$ -director configuration around topological defects is determined by the elastic anisotropy. In a nonpolar SmC film [Figs. 1(a) and 1(b)] the pure bend elastic distortion exists around the  $S = +1$  point defect (so-called bend-type  $S = +1$  topological defect [4]). Formation of this structure is related with the fact that in nonpolar films 2D bend elastic constant  $K_B$  is lower than the constant for splay deformation  $K_S$  [20,24].

In chiral films, symmetry allows the existence of invariant  $K_I (\nabla \times \mathbf{c})$ . The corresponding energy has the form

$$F_{el} = h K_I \int (\nabla \times \mathbf{c})^2 d^2x. \quad (2)$$

The subintegral expression is a full derivative, and  $F_{el}$  can be reduced to boundary integral. In polar films, bend of the  $\mathbf{c}$ -director (splay of polarization) produces the space charges  $\rho(r) = -\text{div}\mathbf{P}$  [23]. The polarization space charge increases the total energy of the bend configuration, in particular, increases the energy of the bend-type topological defects. In other words, polarization charges induce the change of 2D elasticity namely increase the effective bend elastic constant [7]:

$$K_B = K_B^0 + 4\pi h \lambda P^2, \quad (3)$$

where  $K_B^0$  is the bare bend elastic constant in the film without polarization, and  $\lambda$  is the Debye screening length [7]. Equation (3) is valid for  $h < \lambda$ . In polar films  $\lambda$  can be about  $0.7 \mu\text{m}$  [7]. In our investigations, island thicknesses were less than 12 layers (less than  $0.05 \mu\text{m}$ ). So we can assume that  $h$  was less than  $\lambda$ . The magnitude of the effective bend elastic constant  $K_B$  in films with large polarization can become larger than  $K_S$ . This situation ( $K_B > K_S$ ) is realized in our polar films. To minimize the free energy, the topological defect in the SmC\* film becomes splay-type [radial orientation, Figs. 2(a) and 2(b)]. Radial orientation is observed near defects in material with high polarization. In materials with low polarization, the orientation is circular as in nonpolar films. We observed circular orientation around  $S = +1$  defects in a mixture of polar isomers (mixture of 9.6% chiral 11BSMHOB with racemate).

We now focus our attention on a more complex situation, when the defect core is a droplet. The droplets are nucleated in the core of the point topological defects with  $S = +1$  upon heating above the bulk melting temperature. The tangential or radial boundary condition on the droplet-film interface makes droplets topologically equivalent to  $S = +1$  topological defects in a sense of the  $\mathbf{c}$ -director orientation outside the droplets. The  $\mathbf{c}$ -director distribution near a point singularity is determined by the bulk elastic energy. The important difference between a small core and the droplet of micrometer size is linked to the boundary energy of the droplet that can strongly influence

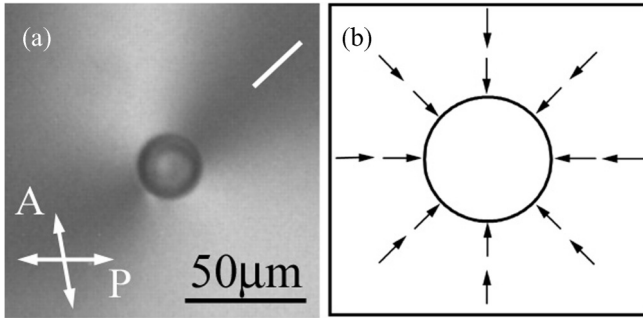


FIG. 3. Modification of the  $\mathbf{c}$ -director field near a cholesteric droplet with topological charge  $S = +1$  in a ferroelectric film. At low temperature tangential boundary conditions on the droplet boundary as in Fig. 2(c) are observed. At high temperature (a) the director at the droplet boundary rotates by  $90^\circ$ , the boundary conditions become radial (b),  $T = 107.6^\circ\text{C}$ . The photograph was made under slightly decrossed polarizers (P, A). The white line in (a) indicates the  $\mathbf{c}$ -director orientation in dark regions. 9BSMHOB.

the bulk  $\mathbf{c}$ -director field. The equilibrium texture corresponds to the global minimum of the sum of elastic, electrostatic, and boundary energy. The anisotropic boundary energy per unit length can be written as  $F_b = 1/2W(\mathbf{c} \cdot \mathbf{n})^2$ , where  $W$  is the anchoring energy on the boundary, and  $\mathbf{n}$  is the direction normal to the droplet boundary [25,26]. In our case, at low temperature the  $\mathbf{c}$ -director is oriented tangentially everywhere at the droplet boundary; i.e.,  $W > 0$ . The tangential boundary condition corresponds to circular streamlines of the  $\mathbf{c}$ -director field near the surface of the droplets. So, droplet nucleation in a nonpolar film does not change the  $\mathbf{c}$ -director configuration [Fig. 1(d)] and does not increase the 2D elastic energy of the film. The tangential alignment was also found near isotropic droplets with defects lying on the isotropic-smectic interface [27]. In ferroelectric films the orientation of the  $\mathbf{c}$ -director around the point defect is radial [Fig. 2(b)], but the boundary condition on the droplet-film interface, like in SmC films discussed above, is tangential. Competition between boundary and bulk  $\mathbf{c}$ -director orientations leads to a change of the initial  $\mathbf{c}$ -director configuration around the droplet. The  $\mathbf{c}$ -director orientation at large distances from the droplet remains nearly the same. However, near the droplet the  $\mathbf{c}$ -director orientation becomes circular. The transitional region near the droplet with a spiral structure is formed [Fig. 2(c)].

Cooling and heating of the polar film lead to dramatic changes of the boundary conditions and the configuration of the  $\mathbf{c}$ -director field around  $S = +1$  droplets. The foregoing  $\mathbf{c}$ -director transformation around a droplet is observed. We start with the low temperature near the SmC\*-N\* transition. As in Figs. 2(c) and 2(d), the  $\mathbf{c}$ -director orientation is tangential on the droplet boundary. Remarkably, at higher temperature the rearrangement of the  $\mathbf{c}$ -director takes place and its orientation on the inclusion boundary becomes radial [Figs. 3(a) and 3(b)]. The white line in Fig. 3(a) shows the  $\mathbf{c}$ -director orientation in the dark region. Dark and bright brushes correspond to regions with perpendicular  $\mathbf{c}$ -director orientation. At low temperature the droplets have a smectic meniscus. When the meniscus consists of smectic layers, the orientation of the  $\mathbf{c}$ -director is parallel to the droplet boundary, as the

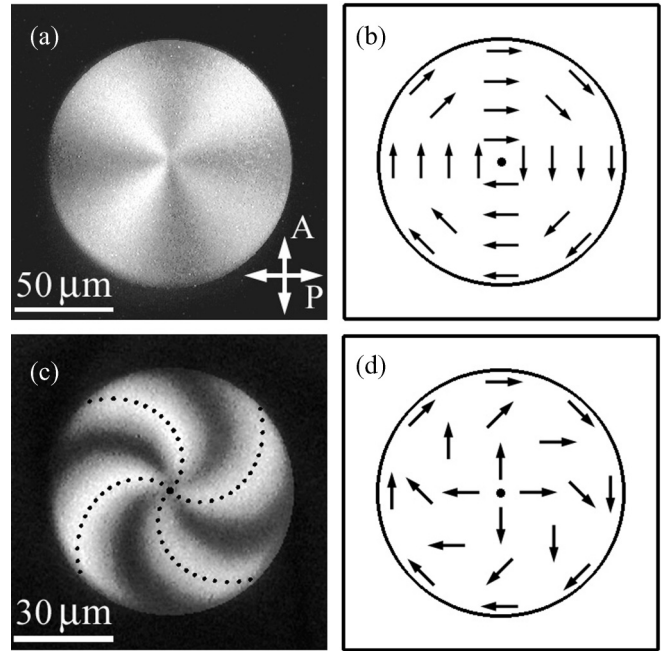


FIG. 4. (a) A nonpolar SmC island with an  $S = +1$  topological defect.  $T = 52.7^\circ\text{C}$ , HOPDOB. (b) A schematic representation of the pure bend  $\mathbf{c}$ -director configuration. (c) A ferroelectric SmC\* island with an  $S = +1$  topological defect. Black dots show the calculated spiral structure for orientations of the  $\mathbf{c}$ -director  $\varphi = \pi/4, 3\pi/4, 5\pi/4,$  and  $7\pi/4$  and  $K_B/K_S = 3.8$ .  $T = 101^\circ\text{C}$ , 9BSMHOB. The dark areas around the islands (a, c) are two-layer films. The photographs are taken in reflection with crossed polarizers (P, A). (d) A schematic representation of the spiral with  $\pi/2$  rotation of the  $\mathbf{c}$ -director.

orientation of the director near an edge dislocation [28]. In our opinion the change of the orientation on heating could be related to the transformation of the structure of the meniscus, when at high temperature it transforms into the cholesteric phase.

Essential transformation of the  $\mathbf{c}$ -director configuration occurs for topological defects or droplets with  $S = +1$  in confined geometry. Figures 4(a) and 4(c) show nonpolar and polar smectic islands in two-layer films (black region around circular islands). Such islands are circular regions thicker than the surrounding film. Smectic islands have strong tangential anchoring at their boundaries. The boundary contains edge dislocations that have lower energy when the  $\mathbf{c}$ -director orients parallel to the dislocation [28]. Topological restrictions require the existence of a topological defect with  $S = +1$  in the island. In nonpolar smectic, the  $\mathbf{c}$ -director field orients circularly both around the core of the defect and near the outer boundary. Four-arm brushes [Fig. 4(a)] correspond to circular orientation of the  $\mathbf{c}$ -director in the whole island.

In ferroelectric films with large polarization circular orientation is observed only in small islands. Clockwise orientation of the  $\mathbf{c}$ -director in polar films along the island boundary was observed in all studied films. Orientation of the  $\mathbf{c}$ -director in large islands near the defect core and on the outer boundary becomes nearly perpendicular, which leads to formation of spiral textures [Fig. 4(c)]. The transition from bend to spiral

configuration takes place at island radius about  $12 \mu\text{m}$ . Radial configuration near the defect has lower energy since in polar films  $K_S < K_B$ . The observed textures in smectic islands correlate with the results obtained by Meyer's [7,18,29–31] and Clark's [32] groups.

We calculated the **c**-director configuration in circular islands using the elastic energy Eq. (1). Let us place the coordinate origin in the island center and introduce an angle  $\psi$  denoting the **c**-director angle with respect to radial orientation. In polar coordinates taking into account axial symmetry, the elastic energy can be written in the form

$$F = \pi h \int (K_S(\cos \psi - \sin \psi \cdot \psi')^2 + K_B(\sin \psi + \cos \psi \cdot \psi')^2) d\eta, \quad (4)$$

where  $\eta = \ln(r/r_0)$ ,  $\psi' = d\psi/d\eta$ ,  $r_0$  is the integration limit for small  $r$ . However, before performing calculations it is worth making some comments about the applicability of expansion Eqs. (1) and (4). The description based on quadratic Frank energy presumes constancy of the order parameter modulus and small spatial variation of the **c**-director orientation. The approach based on quadratic expansion Eqs. (1) and (4) is not valid in the topological defect core. The size of the core  $r_c$  is assumed to be about  $10 \text{ nm}$  [33]. However, in a polar film another size exists  $r_p$  (sufficiently exceeding  $r_c$ ) on which Eqs. (1) and (4) cannot be used even with a renormalized elastic constant  $K_B$ . Equations (1) and (4) in polar films are valid for long-wavelength deformations with wavevector  $q < \lambda^{-1}$  [7]. So in a polar film, one can use the energy in the quadratic form of Eqs. (1) and (4) for  $r_0 > \lambda/2$ , which is sufficiently larger than  $r_c$ . In an island of size essentially larger than the critical size of the transition from circular orientation to spiral one, orientation of the **c**-director near the center, as in the free topological defect, is close to radial. Calculation of the **c**-director orientation was performed for  $\psi = \pi/2$  at the outer boundary and  $\psi = 0$  in the central part of the island at  $r = r_0$ . Dots in Fig. 5 show the orientation of  $\psi$  at different distances from the island center. Dots are results obtained by averaging over the orientation in dark and bright regions in Fig. 4(c). Curves in Fig. 5 are the dependences of  $\psi(r)$  obtained as a result of minimization of energy Eq. (4) for different values of the ratio  $K_B/K_S$  and  $r_0 = 0.5 \mu\text{m}$ . The experimental data are close to the calculated curve 1 for  $K_B/K_S = 3.8$ . In nonpolar smectics  $K_B/K_S$  is about  $0.1\text{--}0.3$  [20,24,34]. Polarization leads to a sufficient increase of the bend elastic constant. Dots in Fig. 4(a) show the calculated positions where the orientation of the **c**-director is  $\varphi = \pi/4, 3\pi/4, 5\pi/4,$  and  $7\pi/4$ ,  $K_B/K_S = 3.8$ .

We observed a nontrivial **c**-director configuration in smectic islands with an  $S = +1$  droplet in its center (Fig. 6). Rotation of brushes from the inner to the outer boundary is by  $180^\circ$ . Figure 6(b) schematically shows the **c**-director configuration corresponding to the texture of Fig. 6(a). The droplet has nucleated in the center of the  $S = +1$  topological defect on heating. In ferroelectric films with high polarization the structure with opposite sense of the **c**-director rotation along the two boundaries is energetically more favorable for  $R_i/R_d \gg 1$  ( $R_i$  and  $R_d$  are island and droplet radii) than the structure with the same sense of the **c**-director rotation [30]. So small droplets have to nucleate with opposite sense of the

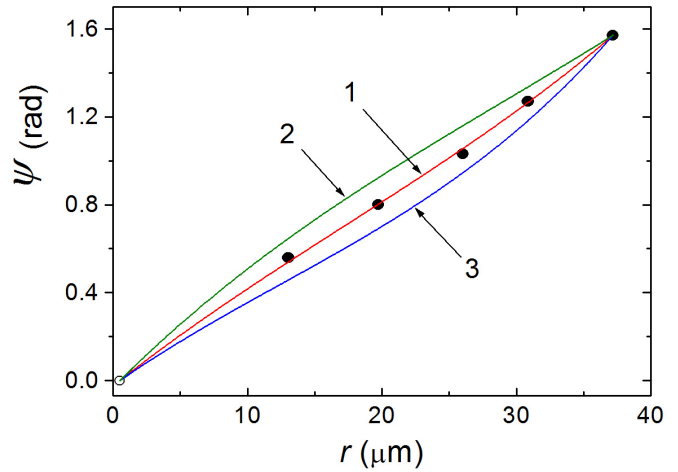


FIG. 5. (Color online) Dots show the orientation of the **c**-director (angle  $\psi$ ) as a function of the distance from the island center obtained using Fig. 4(c). Curves are the calculated dependences of  $\psi(r)$  obtained for different values of the ratio  $K_B/K_S$ : curve 1 for  $K_B/K_S = 3.8$ , curve 2 for  $K_B/K_S = 2.5$ , curve 3 for  $K_B/K_S = 7$ .  $R_i = 37 \mu\text{m}$ ,  $r_0 = 0.5 \mu\text{m}$ .

**c**-director rotation along the inner boundary with respect to director rotation along the outer boundary. Interestingly, when the droplet increases in size the orientation remains unchanged in large droplets, although the same direction of rotation on two boundaries has smaller energy for large droplets. It means that the configuration in Fig. 6(a) is metastable. The previously obtained values of the ratio  $K_B/K_S$  were used to calculate the director orientation in an island with a cholesteric droplet [Fig. 6(a)]. In accordance with the photo [Fig. 6(a)], the boundary conditions were taken  $\psi = \pi/2$  at the outer boundary and  $\psi = -\pi/2$  at the inner boundary. Dots [Fig. 6(a)] are the results of calculation of the spiral structure for  $K_B/K_S = 3.8$  using Eq. (4). As can be seen from the figures, the experimental data are well described by theory. In spite of the opposite direction of the **c**-director rotation around the droplet and along the outer boundary [Fig. 6(a)], encircling the defect

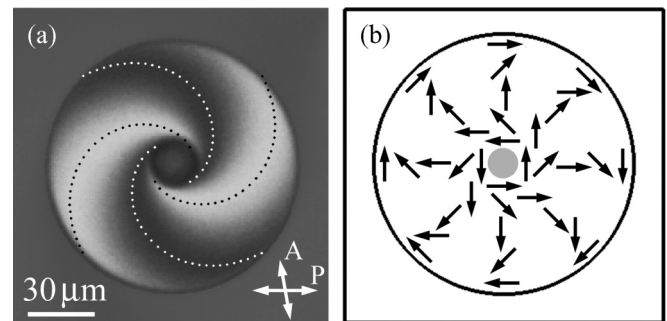


FIG. 6. (a) A ferroelectric  $\text{SmC}^*$  island with a cholesteric droplet corresponding to the topological charge  $S = +1$ .  $T = 104.8^\circ\text{C}$ , 9BSMHOB. Reflection image under slightly decrossed polarizers (P, A). Points are the calculated spiral structure for orientations of the **c**-director  $\varphi = \pi/4, 3\pi/4, 5\pi/4,$  and  $7\pi/4$  and  $K_B/K_S = 3.8$ . (b) A schematic representation of the spiral with rotation of the **c**-director by  $\pi$ .

by any path will result in the same topological charge  $S = +1$ . Lee *et al.* [31] calculated spiral structures in islands for weak anchoring at the radius of the particle in island center. In their experiments, smoke particles were used to create islands. In our experiment, smoke particles were not used; rigid boundary conditions are both at the inner and the outer boundary (Fig. 6).

Different  $\mathbf{c}$ -director configurations near droplets can be classified by two numbers. The first one is the usual topological charge  $S$  of the defect (or of the droplet nucleated in the defect). The second one is the radial number  $m = \Delta\varphi/2\pi$  [29], which describes the radial distribution of the  $\mathbf{c}$ -director. The value of the topological charge  $S$  does not depend on the path of encircling around the defect.  $m$  reflects the orientation of  $\mathbf{c}$ -director in the sample and can differ for the same value of  $S$ . For our experiments it is convenient to define  $\Delta\varphi$  as the difference between  $\mathbf{c}$ -director orientation near the point defect or on the droplet boundary and the orientation of the  $\mathbf{c}$ -director at some distance from the defect. For both pure circular [Figs. 1(a), 1(c), and 4(a)] and pure radial [Fig. 3(a)] configurations,  $m = 0$ . In ferroelectric films we observed the changes of  $m$  by the  $\mathbf{c}$ -director reorientation on the boundary [ $m \approx 1/4$  in Fig. 2(c),  $m = 0$  in Fig. 3(a), and  $m = 1/2$  in Fig. 6(a)].

In summary, in our study we observed manifold director field configurations around droplets in smectic films. The configurations result from a subtle balance between the anisotropy of elasticity, electrostatic energy arising from polarization space charges, surface anchoring, and confined geometry. Orientation of the  $\mathbf{c}$ -director field when a point defect inside an island nucleates a droplet has been studied. In ferroelectric films the transformation of the boundary conditions which results in change of the  $\mathbf{c}$ -director orientation from tangential to radial (rotation by  $90^\circ$  in an  $S = +1$  droplet) was found. This transformation is related to the competition between elastic and boundary energy. In confined geometry the structure with opposite sense of the  $\mathbf{c}$ -director rotation along the inner and outer boundary is reported. The  $\mathbf{c}$ -director configuration in circular islands was calculated and the ratio of the elastic constants  $K_B/K_S$  was estimated. The described phenomena open the way for manipulation of the topological defects and  $\mathbf{c}$ -director field in smectic films.

This work was supported in part by RFBR Grants No. 12-02-33124-mol-a-ved and No. 14-02-01130-a and by the Program of the Presidium of RAS. We thank H. T. Nguyen, A. Babeau, and S. Gineste for synthesis of the liquid crystals.

- 
- [1] P. G. de Gennes and J. Prost, *The Physics of Liquid Crystals*, 2nd ed. (Clarendon Press, Oxford, 1993).
- [2] P. Chaikin and T. C. Lubensky, *Principles of Condensed Matter Physics* (Cambridge University Press, Cambridge, 1995).
- [3] P. Pieranski, L. Bieliard, J.-Ph. Tournelles, X. Leoncini, C. Furtlehner, H. Dumovlin, E. Rion, B. Jouvin, J.-P. Fénerol, Ph. Palaric, J. Heuving, B. Cartier, and I. Kraus, *Physica A* **194**, 364 (1993).
- [4] D. R. Link, N. Chattham, J. E. Maclennan, and N. A. Clark, *Phys. Rev. E* **71**, 021704 (2005).
- [5] P. V. Dolganov, H. T. Nguyen, E. I. Kats, V. K. Dolganov, and P. Cluzeau, *Phys. Rev. E* **75**, 031706 (2007).
- [6] P. V. Dolganov and P. Cluzeau, *Phys. Rev. E* **78**, 021701 (2008).
- [7] J.-B. Lee, R. A. Pelcovits, and R. B. Meyer, *Phys. Rev. E* **75**, 051701 (2007).
- [8] P. Cluzeau, F. Bougrioua, G. Joly, L. Lejcek, and H. T. Nguyen, *Liq. Cryst.* **31**, 719 (2004).
- [9] P. V. Dolganov, H. T. Nguyen, G. Joly, V. K. Dolganov, and P. Cluzeau, *Europhys. Lett.* **78**, 66001 (2007).
- [10] P. V. Dolganov, E. I. Kats, and P. Cluzeau, *Phys. Rev. E* **81**, 031709 (2010).
- [11] P. Cluzeau, M. Ismaili, A. Annakar, M. Foulon, A. Babeau, and H. T. Nguyen, *Mol. Cryst. Liq. Cryst.* **362**, 185 (2001).
- [12] P. Cluzeau, G. Joly, H. T. Nguyen, and V. K. Dolganov, *Pis'ma Zh. Eksp. Teor. Fiz.* **75**, 573 (2002) [*JETP Lett.* **75**, 482 (2002)].
- [13] P. V. Dolganov, K. I. Belov, and V. K. Dolganov, *Pis'ma Zh. Eksp. Teor. Fiz.* **93**, 813 (2011) [*JETP Lett.* **93**, 731 (2011)].
- [14] D. R. Link, J. E. Maclennan, and N. A. Clark, *Phys. Rev. Lett.* **77**, 2237 (1996).
- [15] R. Pindak, C. Y. Young, R. B. Meyer, and N. A. Clark, *Phys. Rev. Lett.* **45**, 1193 (1980).
- [16] D. H. Van Winkle and N. A. Clark, *Phys. Rev. A* **38**, 1573 (1988).
- [17] C. D. Muzny and N. A. Clark, *Phys. Rev. Lett.* **68**, 804 (1992).
- [18] I. Kraus and R. B. Meyer, *Phys. Rev. Lett.* **82**, 3815 (1999).
- [19] P. V. Dolganov, H. T. Nguyen, G. Joly, V. K. Dolganov, and P. Cluzeau, *Europhys. Lett.* **76**, 250 (2006).
- [20] A. Eremin, Ch. Bohley, and R. Stannarius, *Eur. Phys. J. E* **21**, 57 (2006).
- [21] P. V. Dolganov, H. T. Nguyen, G. Joly, V. K. Dolganov, and P. Cluzeau, *Eur. Phys. J. E* **25**, 31 (2008).
- [22] K. Harth, A. Eremin, and R. Stannarius, *Soft Matter* **7**, 2858 (2011).
- [23] C. Y. Young, R. Pindak, N. A. Clark, and R. B. Meyer, *Phys. Rev. Lett.* **40**, 773 (1978).
- [24] P. V. Dolganov and B. M. Bolotin, *Pis'ma Zh. Eksp. Teor. Fiz.* **77**, 503 (2003) [*JETP Lett.* **77**, 429 (2003)].
- [25] A. Rapini and M. Papoular, *J. Phys. (Paris), Colloq.* **30**, C4-54 (1969).
- [26] C. Bohley and R. Stannarius, *Eur. Phys. J. E* **23**, 25 (2007).
- [27] C. Völtz and R. Stannarius, *Phys. Rev. E* **70**, 061702 (2004).
- [28] Y. Hatwalne and T. C. Lubensky, *Phys. Rev. E* **52**, 6240 (1995).
- [29] K.-K. Loh, I. Kraus, and R. B. Meyer, *Phys. Rev. E* **62**, 5115 (2000).
- [30] R. B. Meyer, D. Konovalov, I. Kraus and J.-B. Lee, *Mol. Cryst. Liq. Cryst.* **364**, 123 (2001).
- [31] J.-B. Lee, D. Konovalov, and R. B. Meyer, *Phys. Rev. E* **73**, 051705 (2006).
- [32] A. Pattanaporkratana, C. S. Park, J. E. Maclennan, and N. A. Clark, *Ferroelectrics* **344**, 71 (2006).
- [33] H.-R. Trebin, *Liq. Cryst.* **24**, 127 (1998).
- [34] P. V. Dolganov, P. Cluzeau, and V. K. Dolganov, *Zh. Eksp. Teor. Fiz.* **143**, 1209 (2013) [*JETP* **116**, 1043 (2013)].